Graphene layered systems as a terahertz source with tuned frequency

K. Batrakov* and S. Maksimenko
Institute for Nuclear Problems, Belorussian State University, Bobruiskaya 11, 220050 Minsk, Belarus
(Received 5 October 2016; revised manuscript received 11 April 2017; published 8 May 2017)

The propagation of an electron beam over a graphene/dielectric sandwich structure is considered assuming the distance between the graphene layers in sandwich is large enough to prevent interlayer tunneling. A dispersion equation for the surface electromagnetic modes propagating along graphene sheets is derived and Čerenkov synchronism between a surface wave and a nonrelativistic electron beam is predicted at achievable parameters of the system. Generation frequency tuning is proposed by varying the graphene doping, the number of graphene sheets, the distance between sheets, etc.

DOI: 10.1103/PhysRevB.95.205408

I. INTRODUCTION

Owing to a variety of scientific and technical applications, there is a great need for the development of coherent terahertz radiation sources with a tunable frequency (see, e.g., Refs. [1,2], and references therein). In particular, tunability can be realized in devices utilizing the kinetic energy of moving electrons and transforming it into the energy of the emitted electromagnetic wave [3]. Free-electron lasers (FELs) [4], traveling wave tubes (TWTs), and backward wave oscillators (BWOs) are the well-known devices of such a type. The energy transfer occurs when the parameters of the electron beam moving with velocity $\mathbf{u}$ and the electromagnetic wave meet the synchronism condition (for example, $\omega - \mathbf{ku} = \mathbf{0}$ in the Čerenkov case). By changing the electron velocity, one can smoothly tune the frequency in a wide range. The development of FELs was initiated, in particular, by this feature. However, the electron beam sources are normally optimized for working at a given electron energy and do not allow its easy variation without a considerable drop in efficiency. Instead, tunability could be achieved by exposing the medium which provides the synchronization conditions to the external fields—for example, by varying the undulator magnetic field [4]—but again, this technique appears to be rarely used in practice since the undulator is usually designed for a given operating frequency and its efficiency significantly drops with deviations.

In the case of a Čerenkov-type emitter [5], the radiation frequency depends *also* on the electrodynamic parameters of the medium, thus providing alternative means of resonant frequency tuning. Among the different possibilities, graphene and carbon nanotubes (CNTs) are very promising materials from this point of view since there are well known and rather facile methods to vary their constitutive parameters over a wide range. In particular, the well-developed methods of graphene doping that include electrostatic doping allow a smooth alteration of the surface conductivity [6]. An analogous effect is reported in doped CNTs [7,8]. Besides, it has been shown that carbon nanotubes and graphene can considerably slow down the surface electromagnetic wave [9,10], thus providing better conditions for the synchronization of the electron beam and electromagnetic surface wave.

The Čerenkov mechanism of the generation of coherent stimulated radiation in graphene and carbon nanotubes was theoretically investigated in Refs. [10–15], demonstrating the realizability of nanotube-based nano-TWTs and nano-FELs at realistic parameters of the CNTs and electron beams [14]. The mechanism of the generation and amplification of plasmon oscillations in graphene by optical or electrical pumping has been discussed in the literature [16–21]. The efficiency of emission and the influence of the quantum recoil effect on Čerenkov emission by hot electrons in graphene were studied in Refs. [22,23]. The possibility of terahertz emission in CNTs imposed on transverse and axial electric fields due to electric-field-induced heating of the electron gas has been revealed in Refs. [24–28]. A periodical system of graphene nanoribbons has been proposed as the Čerenkov medium with the regulation of generation frequency by the width of the nanoribbon, the spatial period, and the applied voltage [29,30]. A similar approach exploiting the periodic dielectric substrate underlying the graphene sheet has been developed in Refs. [31,32]. A variant that is analogous to Čerenkov radiation due to the excitation of dipole polarization in the array of nanotubes, which leads to current generation with a superluminal profile, is considered in Refs. [33,34].

The unique physical properties of graphene, either as a plane or rolled up into a cylinder, are featured because not only can an external electron beam be used for the excitation of surface waves but also graphene's own π electrons can be used [10,14,29]. There are several reasons in favor of such a generation scheme: First, graphene and nanotubes support an extraordinarily large continuous electric current density, $>10^8$ A/cm^2, without degradation (see, e.g., Refs. [35–37]). Then, a macroscopically large ballistic length (up to several hundred microns) in graphene and the nanotubes is reported [38–41]. For example, an about 16 μm long electron ballistic transport in graphene nanoribbons has been observed recently [42]. Therefore, electrons can emit coherently from this macroscopic length. The physical basis of such a high ballisticity is in the Dirac nature of the graphene carriers and the Klein paradox [43,44], which helps one to overcome the potential barriers. Lastly, metallic CNTs exhibit a strong, as large as 50–100 times, slowing down of the surface electromagnetic waves [9]. In single-layer graphene this quantity appears to be smaller, but below we show that this problem can be resolved by using a slow acoustic mode in a multilayered structure due to the coupling of plasmon-polariton modes of

*kgbatrakov@gmail.com

different layers [10]. A similar effect can be achieved by the hybridization of the graphene plasmon with its mirror image in the metal plate disposed near the graphene layer that leads, in particular, to a strongly confined asymmetric mode [45,46]. Thus, as it has been stressed in Ref. [14], the combination in graphene and CNTs of three key properties, (i) the ballisticity of the electron flow over a typical length, (ii) an extremely high current-carrying capacity, and (iii) a strong slowing down of the surface electromagnetic waves [9], allows us to propose them as candidates for the development of nanosized Černekov-type emitters. As our estimates show [14], an electron mean free path as large as tens of microns would be enough to provide coherent emission and reach the above stated goal. However, the practical realization of such a large ballistical transport is a complicated task and, in any case, is inconsistent with the high current density.

Alternatively, traditional Černekov and Smith-Purcell generation schemes can be utilized, when an external electron beam moves synchronously with the excited surface wave over the graphene surface over a distance sufficient to neglect electron collisions with the carbon atoms. A later condition allows one to exclude the negative role of the electrons' multiple scattering, which destroys Čerenkov synchronism. To provide the necessary slowing down, we propose to make use of a sandwich structure consisting of parallel noninteracting graphene layers. In Ref. [10] we have shown that in two spatially separated graphene layers, one of the surface plasmonic modes can be significantly slowed down, up to the velocity of the graphene π electrons. Moreover, a different mechanism of frequency tuning appears, exploiting the variation in the interlayer distance. Recently [47,48], we have demonstrated a strong graphene interaction with radiation. In particular, a free-standing single graphene layer can absorb up to 50% of the exposing radiation intensity in the microwave and terahertz frequency ranges. This percentage can be significantly increased under a corresponding choice of substrate. From the Einstein rules, it follows that the inverse process, i.e., stimulated radiation emission, can proceed equally effectively.

In the present paper we study the excitation of surface waves propagating in graphene sandwich structures and resonantly interacting with an electron beam, aiming at revealing the generation conditions and methods of smooth frequency tuning by variations in the system parameters. The remainder of the paper is organized as follows. In Sec. II the formulation of the problem and basic equations are presented. A solution of the boundary-value problem for a single-layer graphene sheet, the possibility for an electromagnetic wave to slow down, and frequency tuning in that case is presented in Sec. III. Section IV presents results concerning the surface electromagnetic wave in a two-layer graphene system, a slowing down of an enhanced wave for the acoustical mode, and an addictive change in the effective chemical potential for the optical mode. Both these effects give the possibility to regulate the generated frequency and resonance electron beam energy. A dispersion equation for a graphene system with an external electron beam is presented in Sec. V. The solution of this equation gives us an increment of instability and estimation that is required for generation parameters. Section VI contains an analysis concerning the possibilities of generation and frequency tuning based on previous calculations, and conclusion remarks.

II. BASIC EQUATIONS

Consider an electron beam propagating along the x axis parallel to a graphene sheet or multilayer graphene sandwich structure comprising graphene sheets separated by layers of a medium with dielectric functions ε_i. The index i marks the double-layer graphene+underlying medium in the sandwich (see Fig. 1). On its way over the sandwich, the beam interacts with the surface electromagnetic wave retained by the graphene structure. For coherent radiation generation, the beam motion should be synchronized with the electromagnetic wave on the beam propagation length over the structure. In particular, for the Čerenkov emission mechanism, the electron beam velocity must coincide with the phase velocity $v_{\rm ph}$ of the electromagnetic wave. That is, since the electron velocity is smaller than the speed of light, the slowing down of the surface wave is a necessary condition for synchronization.

Let us examine the propagation of surface waves along the sandwich in free space, assuming the distances between the graphene layers to be large on the atomic scale and, therefore, neglecting electron interlayer tunneling in the sandwich. Further, we follow the procedure developed in Refs. [47–49]. The eigenwaves under study satisfy the Maxwell equations, the boundary conditions at the graphene surfaces in each layer, and the condition that there are no exterior current sources at infinity. From the Maxwell equations we express the field of the transverse magnetic (TM) wave in a piecewise continuous form,

$$H_y^{(i)} = e^{iqx}\left(c_1^{(i)} \exp\left\{ik_z^{(i)}z\right\} + c_2^{(i)} \exp\left\{-ik_z^{(i)}z\right\}\right). \qquad (1)$$

Here, the z axis is perpendicular to the graphene layers, $k_z^{(i)} = \sqrt{\omega^2\varepsilon_i/c^2 - q^2}$ is the z projection of the wave vector in the ith layer, and $\mathbf{q}$ is the tangential component of the wave vector. Further, we assume $\varepsilon_i = 1$. Generalization of the case $\varepsilon_i \neq 1$ can be easily performed and, what is important, it does not create essential changes. To find the surface eigenmodes we need to determine the unknown coefficients $c^{(i)}$. The boundary conditions state the continuity of the tangential component of the electric field on the graphene surface while the tangential component of the magnetic field undergoes a discontinuity proportional to the surface current $\mathbf{j}_t$ excited in graphene

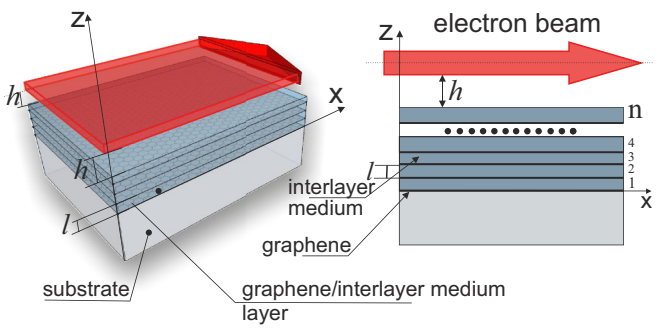

FIG. 1. Geometry of the problem.

[47–49],

$$\mathbf{H}(z_i + 0) - \mathbf{H}(z_i - 0) = \frac{4\pi}{c}[\mathbf{j}_t(z_i) \times \mathbf{n}]. \quad (2)$$

Here, $\mathbf{n}$ is the unit vector along the z axis. As it has been shown in Ref. [49], the surface current excited in the graphene layer is related to the electric field by

$$\mathbf{j}_t = \sigma \mathbf{E}_t = \alpha g_s g_v \frac{T}{\pi\hbar} \ln\left[2\cosh\left(\frac{\mu}{2T}\right)\right] \frac{ic}{\omega + i\Gamma} \mathbf{E}_t, \quad (3)$$

where σ is the sheet conductivity of the monolayer graphene, μ is the chemical potential of the electron subsystem, T is the temperature in energy units, Γ is the broadening parameter (collision frequency), and α is the fine structure constant. In further calculations we assume $\Gamma \sim 10$ THz, in accordance with our previous experiments on electromagnetic radiation absorption in graphene sandwich structures [47,48]. Note that in our approach any deviations of graphene from idealness (defects, doping, strains, nonhomogeneities, etc.) are taken into account by variation of the chemical potential and broadening parameter Γ.

The coefficients g_s and g_v are due to spin and valley degeneracies [49] and for graphene it can be accepted that both are equal to 2. In Eq. (3) we only restrict ourselves to intraband transitions. At realistic values of the chemical potential this is correct for the terahertz and microwave frequency ranges and inapplicable in optical and near-infrared (NIR) ranges where the interband transitions come into play. If the chemical potential proves to be less than the operating frequency, the interband transitions should also be accounted for, even at low frequencies. However, to reach such a situation, special efforts are required during graphene synthesis and storage [50].

III. SURFACE WAVES IN A SINGLE-LAYER SYSTEM

Applying the procedure described above to the sandwich structure consisting of n layers, we arrive at a homogeneous system of $2n$ linear equations for $2n$ coefficients $c_{1,2}^{(i)}$. A dispersion equation of the system arises when we set the determinant of the system equal to zero and determine the frequency dependence of the surface-wave wave vector. For a single graphene layer the system comprises two equations for two coefficients,

$$c_2 + c_1 = 0, \quad c_2(1 + \sigma_0) - c_1 = 0. \quad (4)$$

Here, $\sigma_0 = (4\pi/\omega)k_z\sigma$ is a dimensionless parameter with σ given by Eq. (3) under the assumption $g_s, g_v = 2$. Assuming a chemical potential considerably exceeding the temperature, from (4) it follows that

$$\frac{2\mu\alpha}{\hbar\omega} \frac{\sqrt{q^2c^2 - \omega^2}}{\omega + i\Gamma} = 1, \quad (5)$$

which describes the dispersion of the surface electromagnetic wave propagating in graphene. Dispersion equation (5) leads to

$$q^2c^2 = \omega^2 + \left[\frac{\hbar\omega(\omega + i\Gamma)}{2\mu\alpha}\right]^2. \quad (6)$$

This equation demonstrates the frequency dependence of the surface-wave wave vector that is characteristic for degenerated two-dimensional (2D) quantum systems. In the case of potential fields, when we can neglect the first term on the right-hand side of Eq. (6), we arrive at the dependence [51] $q \sim \omega^2$ or $\omega \sim \sqrt{q}$. Note that such a dependence drastically differs from the dependence inherent in the three-dimensional (3D) case, where the eigenfrequency is proportional to the Langmuir plasma frequency and does not depend on the wave vector [52]. The specific dispersion law admits a strong slowing down of surface waves in 2D systems. The slowing down of surface waves at different μ is illustrated in Fig. 2. It is seen that the effect can vary in a wide range of values depending on the frequency and chemical potential.

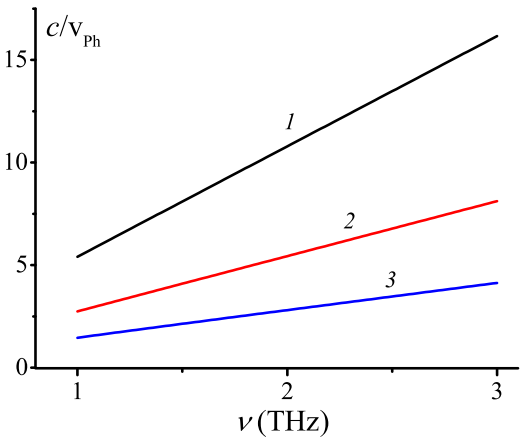

FIG. 2. Slowing down of the phase velocity for a surface wave in an isolated graphene layer for different values of the chemical potential: (1) $\mu = 0.05$ eV, (2) $\mu = 0.1$ eV, (3) $\mu = 0.2$ eV.

The dependence of the Čerenkov resonant frequency (the frequency corresponding to the synchronism condition) ν on the chemical potential is depicted in Fig. 3 at different values of the electron beam energy. Figure 4 demonstrates the variation in the Čerenkov resonant frequency by changing the electron beam energy. Calculations were made for typical values of the chemical potential, $\mu = 0.1$ and 0.2 eV.

In the above analysis we considered the TM wave, whose magnetic field vector is coplanar with graphene and the wave

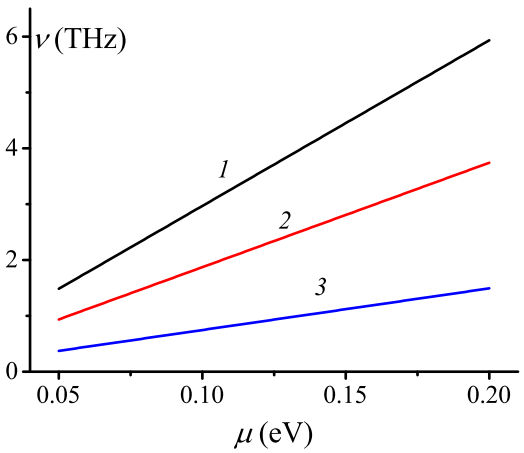

FIG. 3. Čerenkov resonant frequency vs chemical potential at an electron beam energy of (1) 4 keV, (2) 10 keV, and (3) 60 keV.

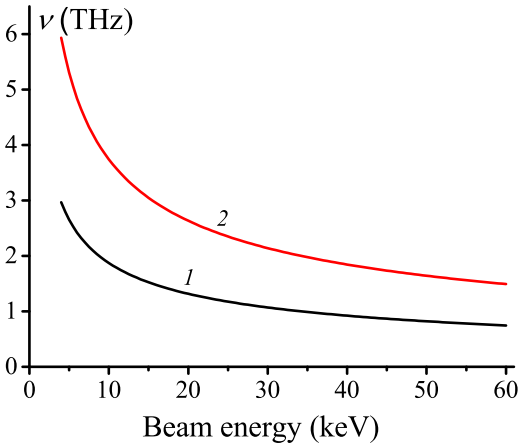

FIG. 4. Čerenkov frequency dependence on the electron beam energy. Chemical potential (1) $\mu = 0.1$ eV and (2) $\mu = 0.2$ eV.

vector is normal to the magnetic field. Analogously, the boundary conditions can be stated for the transverse electric (TE) wave and a corresponding dispersion equation can be obtained,

$$\frac{4\mu\alpha}{\hbar\sqrt{q^2c^2-\omega^2}}\frac{\omega}{\omega+i\Gamma}=-2. \tag{7}$$

See (5) for a comparison. Since the TE wave can exist only when the real part of $\sqrt{q^2c^2-\omega^2}$ is positive, from (7) one can conclude that graphene does not support TE waves in the frequency range under consideration. The excitation of TE waves in an isolated graphene layer is possible at much higher frequencies when the contribution of the interband transitions becomes significant [53].

IV. SURFACE WAVES IN A DOUBLE-LAYER SYSTEM

A double-layer graphene system can be used for the generation of Čerenkov radiation by an electron beam [10]. The advantage achieved by graphene doubling is the appearance of an acoustic mode among the plasmon oscillations inherent in the system. This mode's frequency is proportional to the difference in frequencies of the plasmonic oscillations in the layers. As a result, the phase velocity of this wave appears to be much less than that achievable in monolayers. Owing to such a large slowing down, one can meet Čerenkov synchronism even for graphene π electrons whose velocity is ≈ 300 less than the speed of light.

It should be noted that Eq. (3) for surface conductivity deduced in Ref. [49] holds true only if $\omega \gg q v_F$. If this condition is not valid, a more precise expression for conductivity should be applied [see Eq. (39) in Ref. [10]],

$$\sigma' = \alpha g_s g_v \frac{T}{\pi\hbar}\log\left[2\cosh\left(\frac{\mu}{2T}\right)\right]\frac{ic(\omega+i\Gamma)}{v_F^2q^2} \times \frac{(\omega+i\Gamma)-\left[(\omega+i\Gamma)^2-v_F^2q^2\right]^{1/2}}{\left[(\omega+i\Gamma)^2-v_F^2q^2\right]^{1/2}}. \tag{8}$$

Here, v_F is the π-electron velocity at the Fermi level. In the case $\omega \gg v_F q$, Eq. (8) is reduced to (3).

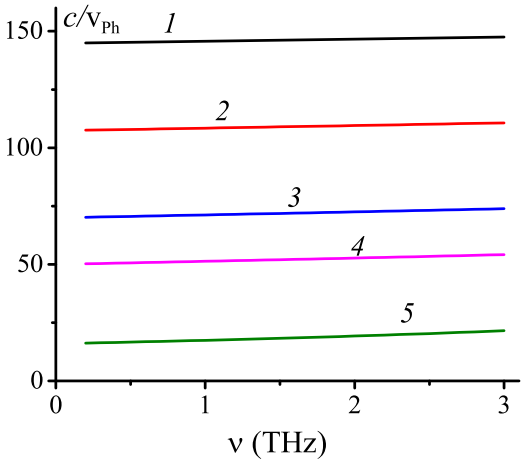

FIG. 5. Slowing down of the phase velocity for the acoustic mode in a structure with two graphene layers. In curves 1–5, the distances between layers are 10 nm, 20 nm, 50 nm, 100 nm, and 1 μm, respectively. The chemical potential in all cases is $\mu = 0.1$ eV.

Let us analyze the surface electromagnetic modes in two graphene layers separated by a distance l. The magnetic field of the TM wave can be written as

$$H_y = \exp\{iqx\} \times \begin{cases} a\exp\{-ik_z z\}, & z<0, \\ c_1\exp\{ik_z z\}+c_2\exp\{-ik_z z\}, & 0<z<l, \\ d\exp\{ik_z(z-l)\}, & z>l. \end{cases} \tag{9}$$

In the regions before ($z < 0$) and after ($z > l$) the structure, system (9) contains only waves exponentially decaying with distance from graphene. The boundary conditions allowing the evaluation of the four coefficients a,d,c_1,c_2 are given by

$$\begin{aligned} &c_1 - c_2 + a = 0, \\ &c_1 + c_2 - a(1+\sigma_0') = 0, \\ &c_1\exp\{-\sqrt{q^2-\omega^2/c^2}\,l\} \\ &\quad - c_2\exp\{\sqrt{q^2-\omega^2/c^2}\,l\} - d = 0, \\ &c_1\exp\{-\sqrt{q^2-\omega^2/c^2}\,l\} \\ &\quad + c_2\exp\{\sqrt{q^2-\omega^2/c^2}\,l\} - d(1+\sigma_0') = 0, \end{aligned} \tag{10}$$

where, as in the previous section, $\sigma_0' = (4\pi/\omega)k_z\sigma'$ and σ' is given by Eq. (8) under the assumption $g_s, g_v = 2$. The resulting dispersion equation,

$$2 + \sigma_0' \pm \sigma_0'\exp\{-\sqrt{q^2-\omega^2/c^2}\,l\} = 0, \tag{11}$$

manifests the appearance of optical and acoustic modes (upper and lower signs, respectively). At distances l much less than the wavelength, the acoustic mode slows down much faster. This is because the terms proportional to conductivity in (11) are mutually suppressed in that case. Thus, in the acoustic mode, the wave number q must be sufficiently large in order to satisfy the dispersion equation.

Figure 5 presents the phase velocity dependence of the surface asymmetric electromagnetic mode on frequency.

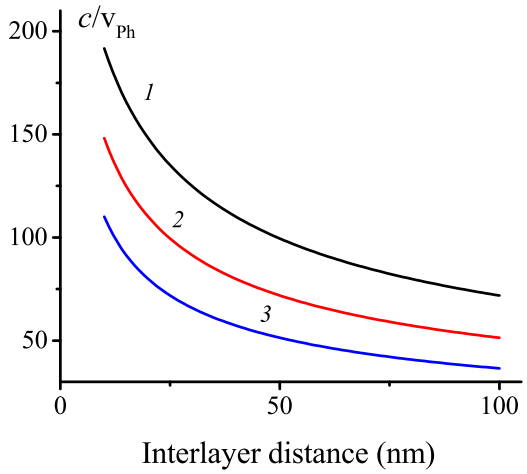

FIG. 6. Slowing down of the acoustic mode as a function of interlayer distance in a double graphene structure at different values of the chemical potential: $\mu = 0.05$ (curve 1), 0.1 (curve 2), and 0.2 (curve 3).

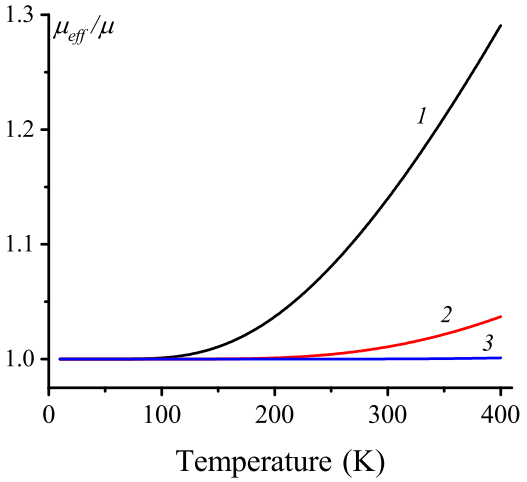

FIG. 7. Temperature dependence of the effective chemical potential for different values of the chemical potential: $\mu = 0.05$ (curve 1), 0.1 (curve 2), and 0.2 (curve 3).

Comparing the curves in this plot with curve 2 from Fig. 2, which has been plotted for a single layer at the same value of the chemical potential $\mu = 0.1$ eV, one can see that the acoustic mode slows down much faster in a double-layer structure than in monolayer graphene. Figure 5 also demonstrates a weak frequency dependence of the slowing down factor in the range considered. On the contrary, the dependence of this factor on interlayer distance is essential (see Fig. 6). This gives us a tool to control the effect by varying the distance.

There is also an optical mode in the double-layer structure under consideration ["+" in (11)]. When the wavelength exceeds significantly the interlayer distance, the dispersion equation of the optical mode differs from the single-layer case in that only the chemical potential should be doubled in all expressions. In particular, this means that the slowing down of this mode is less than in a single graphene layer. When the interlayer distance is considerably less than the wavelength, it can be easily seen that for the optical mode which corresponds to the sign "+" in (11), the effective sheet conductivity is doubled as compared to the case of monolayer graphene. An analogous effect holds true for a sandwich graphene structure with more than two layers. For this case, the effective conductivity is equal to the sum of the layer conductivities. Such an additivity has been observed experimentally in the study of electromagnetic wave transmission through sandwich graphene structures [47,48].

Note that in the above consideration we restricted ourselves to the case $\mu \gg T$. When this inequality is violated, the system can be described by the effective chemical potential

$$\mu_{\text{eff}} = 2T \log\left[2\cosh\left(\frac{\mu}{2T}\right)\right], \tag{12}$$

as it can easily be deduced from (3) and (8). Figure 7 shows the temperature dependence of the ratio μ_{eff}/μ for different values of the chemical potentials. One can see that temperature has a slight influence on the ratio for $\mu > 0.1$ eV up to the poly(methyl methacrylate) (PMMA) melting point, which is why in our transmission/absorption experiments with chemical vapor deposition (CVD)-grown graphene [47,48], where the chemical potential was estimated as $\mu \sim 0.14$–0.17 eV, we did not observe a temperature dependence. "Purer" graphene is expected to be more sensitive to temperature changes.

V. DISPERSION EQUATION IN GRAPHENE STRUCTURES IN THE PRESENCE OF AN ELECTRON BEAM

Let the electron beam of width δ propagate on a distance h from a two-layer graphene structure. The dispersion equation can be derived in the manner described in the previous section. The difference consists in the appearance of an additional region occupied by an electron beam. In this region, the z projection of the wave vector is given by

$$k_{bz} = k_z\sqrt{1 - \frac{\omega_l^2}{\gamma^3(\omega - qu)^2}}, \tag{13}$$

where $\omega_L = \sqrt{4\pi e^2 n_e/m_e}$ is the Langmuir frequency of the electron beam and $\gamma = 1/\sqrt{1 - u^2/c^2}$ its Lorentz factor, u is the velocity of electrons, n_e is the electron density, and e and m_e are the electron charge and mass. The system of boundary conditions in this case is discussed in the Appendix. It leads to the following dispersion equation,

$$I_b = -\frac{(2+\sigma_0')^2 - (\sigma_0')^2\exp\{-2\sqrt{q^2 - \omega^2/c^2}\,l\}}{\sigma_0'[2 + \sigma_0' + \exp\{-2\sqrt{q^2 - \omega^2/c^2}\,l\}(2 - \sigma_0')]}, \tag{14}$$

where

$$I_b = \exp(2ik_z h) \times \frac{\left(k_{bz}^2 - k_z^2\right)\{\exp(ik_{bz}\delta) - \exp(-ik_{bz}\delta)\}}{(k_{bz} - k_z)^2\exp(ik_{bz}\delta) - (k_{bz} + k_z)^2\exp(-ik_{bz}\delta)}.$$

It is obvious that in the case when the distance between the layers significantly exceeds the distance of the surface-wave dumping, the above dispersion equation is reduced to the equation for a single layer. Mathematically, this is achieved

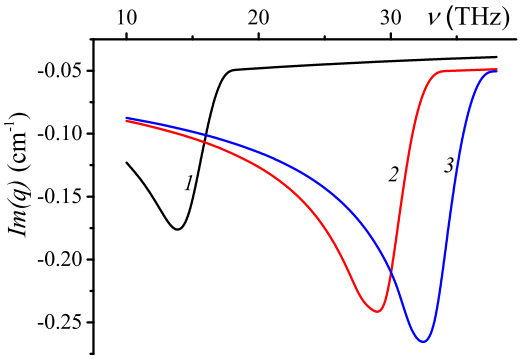

FIG. 8. Frequency dependence of the instability increment [Im(q)] for (1) four, (2) eight, and (3) nine graphene layers with the chemical potential of a single layer, $\mu = 0.2$ eV. Electron beam energy $E = 10$ keV, $\Gamma = 10$ THz.

by neglecting small exponential terms in the numerator and denominator in the right-hand side of (14).

As an example, in Fig. 8 we depict the instability increment (imaginary part of the surface-wave tangential wave number q) as a function of frequency. The negativity of the increment is a necessary condition to start generation. In the figure we compare the frequency dependencies for sandwich structures with four, eight, and nine graphene layers at $\mu = 0.2$ eV in each layer. All curves are characterized by pronounced minima at the Čerenkov resonant frequencies (generation frequencies) with the linewidths dictated by the broadening parameter. These frequencies appear to be in the THz range and significantly shift to the short-wave side with the number of graphene layers. The increments grow in absolute values with the number of graphene layers also. The maximal absolute values of the instability increments presented in Fig. 8 show us that a strong amplification regime can be realized already at an interaction length of the order of several centimeters. At smaller lengths, the incorporation of feedback (for example, a mirror) into the system allows one to achieve generation in a weak-coupling regime.

Figure 9 demonstrates the increment frequency dependencies for monolayer graphene at a smaller electron beam energy and two different chemical potentials. In this case the

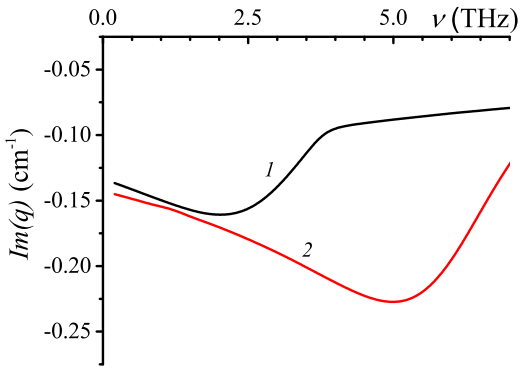

FIG. 9. Frequency dependence of the instability increment [Im(q)] for a single graphene layer. Electron beam energy $E = 4$ keV, and the chemical potential is (1) $\mu = 0.1$ eV and (2) $\mu = 0.2$ eV.

generation frequency is reduced to several terahertz with a simultaneous decrease in the absolute value of the increment. Thus, a multilayer graphene sandwich provides us with much better generation conditions as compared to the monolayer and admits resonant frequency tuning.

VI. CONCLUSION

In the present paper, we have studied the propagation in graphene sandwich structures of surface waves excited by an electron beam moving over the sandwich surface. We have demonstrated the existence in the multilayered structure of a strongly slowed down acoustic mode which allows synchronization of the beam and the surface wave at a much lower beam energy. Moreover, smooth frequency tuning becomes possible by varying the system parameters, such as the beam energy, chemical potential, and interlayer distance.

At a given beam energy the frequency can be smoothly tuned by varying the chemical potential μ by means of electrostatic doping (see Fig. 3). At a fixed chemical potential the tuning is attained by a variation in the electron beam energy, as is demonstrated in Fig. 4. If the graphene sandwich structure allows alteration of the interlayer distance, tuning of the spectrum can be realized even at a fixed chemical potential and beam energy (see Fig. 5). This is because in multilayered graphene structures there are electromagnetic modes whose phase velocities can be both essentially smaller and exceed the surface-wave phase velocity reachable in single-layer graphene. All the factors mentioned allow one to match the electron beam energy, the chemical potential, and the interlayer distance (and number of layers) to synchronize the electron beam and surface electromagnetic wave at a fixed frequency, while an external electrostatic field (electrostatic doping) provides an additional possibility for fine frequency tuning.

It should be emphasized that the graphene layers in the sandwich do not necessarily have to be whole. In order to provide an interaction of the electron beam with the graphene on a length of several centimeters, it is sufficient to have a mosaic surface comprising disoriented in-plane graphene blocks. Moreover, since cylindrical and tubular beams are widespread in electronic engineering, the planar geometry considered in the present paper (see Fig. 1) can be easily rearranged to be cylindrical by, for example, stacking graphene layers on a cylinder.

Thus, based on our analysis, we can conclude that multilayered graphene/dielectric structures with negligible interlayer tunneling provide enhanced conditions for terahertz Čerenkov radiation generation excited by an external nonrelativistic electron beam. Different methods for the generation of frequency tuning can be realized by varying the graphene doping, the number of graphene sheets, the distance between sheets, etc.

ACKNOWLEDGMENTS

This publication is based on work supported by a grant from the U.S. Air Force under Agreement No. FA9550-15-D-0003. The authors also acknowledge support from EU FP7 Project No. FP7-612285 CANTOR and EU Horizon 2020 Project No. H2020-644076 CoExAN.

APPENDIX: ACCOUNTING OF THE ELECTRON BEAM

Consider electron beams propagating over some plane structure (see Fig. 1). As a further consideration, we make use of the procedure developed in Ref. [54]. Linealized equations describing the electron beam dynamics are well known and given by

$$\frac{\partial \delta v_x}{\partial t} + u\frac{\partial \delta v_x}{\partial x} = \frac{e}{m\gamma^3}E_x,$$
$$\frac{\partial \delta n}{\partial t} + \frac{\partial}{\partial x}(n_0 \delta v_x + u\delta n) = 0. \tag{A1}$$

A Fourier transform of (A1) leads to

$$\left(k_{bz}^2 c^2 - \omega^2\right)E_x - q k_{bz} c^2 E_z = -\frac{\omega_L^2 \omega^2}{\Delta^2 \gamma^3}E_x,$$
$$-q k_{bz} c^2 E_x + (q^2 c^2 - \omega^2)E_z = 0, \tag{A2}$$

which gives the dispersion equation as follows

$$k_b^2 c^2 - \omega^2 = \frac{\omega_L^2}{\Delta^2 \gamma^3}(q^2 c^2 - \omega^2), \tag{A3}$$

where $k_b^2 = q^2 + k_{bz}^2$ and $\Delta = \omega - qu$. Solutions of this equation are given by (13). Boundary conditions for the electromagnetic wave (1) interacting with an electron beam are produced by analogy with the case considered in Secs. III and IV by imposing conditions on the tangential components of the electric and magnetic fields on the boundaries. The only difference is that in the beam, the following relation, dictated by the Maxwell equation

$$E_x = \frac{k_{0z}^2 c}{\omega k_{bz}}H_y, \tag{A4}$$

is used for tangential components of the electric and magnetic fields. Particulary, for an electron beam with a thickness δ propagating over two-layer graphene over a distance h, we have a system for eight coefficients. Two of them, a_1 and a_2, correspond to regions below the structure and above the beam, respectively, while the coefficients $c_{1,2}$ and $d_{1,2}$ describe waves inside a two-layer structure and between the structure and beam. Finally, the coefficients $f_{1,2}$ correspond to two counterpropagating waves in the beam,

$$H_y = \exp\{iqx\}$$
$$\times \begin{cases} a_1 \exp\{-ik_z z\}, & z < 0, \\ c_1 \exp\{ik_z z\} + c_2 \exp\{-ik_z z\}, & 0 < z < l, \\ d_1 \exp\{ik_z (z-l)\} & \\ \quad + d_2 \exp\{-ik_z (z-l)\}, & l < z < h, \\ f_1 \exp\{ik_{bz} z\} + f_2 \exp\{-ik_{bz} z\}, & h < z < h+\delta \\ a_2 \exp\{ik_z z\}, & z > h+\delta. \end{cases}$$

Assuming the determinant of this linear system to be zero, we arrive at Eq. (14).

[1] R. A. Lewis, J. Phys. D **47**, 374001 (2014).
[2] A. Pawara, D. Sonawanea, K. Erandea, and D. Derleb, Drug Invent. Today **5**, 157 (2013).
[3] A. Gilmour, *Klystrons, Traveling Wave Tubes, Magnetrons, Cross-Field Amplifiers, and Gyrotrons* (Artech House, Norwood, MA, 2011).
[4] T. Marshall, *Free-Electron Lasers* (Macmillan, New York, 1985).
[5] J. E. Walsh, T. C. Marshall, and S. P. Schlesinger, Phys. Fluids. **20**, 709 (1977).
[6] K. Novoselov, A. Geim, S. Morozov, D. Jiang, Y. Zhang, S. Dubonos, I. Grigorieva, and A. Firsov, Science **306**, 666 (2004).
[7] A. M. Nemilentsau, M. V. Shuba, G. Y. Slepyan, P. P. Kuzhir, S. A. Maksimenko, P. N. D'yachkov, and A. Lakhtakia, Phys. Rev. B **82**, 235424 (2010).
[8] M. A. Kanygin, O. V. Sedelnikova, I. P. Asanov, L. G. Bulusheva, A. V. Okotrub, P. P. Kuzhir, A. O. Plyushch, S. A. Maksimenko, K. N. Lapko, A. A. Sokol *et al.*, J. Appl. Phys. **113**, 144315 (2013).
[9] G. Y. Slepyan, S. A. Maksimenko, A. Lakhtakia, O. Yevtushenko, and A. V. Gusakov, Phys. Rev. B **60**, 17136 (1999).
[10] K. Batrakov, V. Saroka, S. Maksimenko, and C. Thomsen, J. Nanophotonics **6**, 061719 (2012).
[11] K. Batrakov, P. Kuzhir, and S. Maksimenko, Proc. SPIE **6328**, 63280Z (2006).
[12] K. Batrakov, P. Kuzhir, and S. Maksimenko, Physica E **40**, 2370 (2008).
[13] K. Batrakov, P. Kuzhir, and S. Maksimenko, Physica E **40**, 1065 (2008).
[14] K. G. Batrakov, S. A. Maksimenko, P. P. Kuzhir, and C. Thomsen, Phys. Rev. B **79**, 125408 (2009).
[15] K. Batrakov, O. Kibis, P. Kuzhir, C. Rosenau, and M. Portnoi, J. Nanophotonics **4**, 041665 (2010).
[16] M. Jablan, M. Soljacic, and H. Buljan, Proc. IEEE **101**, 1689 (2013).
[17] V. Ryzhii, V. Ryzhii, and T. Otsuji, J. Appl. Phys. **101**, 083114 (2007).
[18] V. Ryzhii, A. Dubinov, T. Otsuji, V. Mitin, and M. S. Shur, J. Appl. Phys. **107**, 054505 (2010).
[19] A. Dubinov, V. Aleshkin, V. Mitin, T. Otsuji, and V. Ryzhii, J. Phys.: Condens. Matter **23**, 145302 (2011).
[20] V. Ryzhii and V. Ryzhii, Jpn. J. Appl. Phys. **46**, L151 (2007).
[21] F. Rana, IEEE Trans. Nanotechnol. **7**, 91 (2008).
[22] F. J. G. de Abajo, ACS Nano **7**, 11409 (2013).
[23] I. Kaminer, Y. T. Katan, H. Buljan, Y. Shen, O. Ilic, J. Lopez, L. Wong, J. Joannopoulos, and M. Soljacic, Nat. Commun. **7**, 11880 (2016).
[24] O. V. Kibis and M. E. Portnoi, Tech. Phys. Lett. **31**, 671 (2005).
[25] O. V. Kibis, D. G. W. Parfitt, and M. E. Portnoi, Phys. Rev. B **71**, 035411 (2005).
[26] O. V. Kibis, M. R. da Costa, and M. E. Portnoi, Nano Lett. **7**, 3414 (2007).
[27] K. Batrakov, O. Kibis, P. Kuzhir, S. Maksimenko, D. C. M. Rosenau, and M. Portnoi, Physica B **405**, 3054 (2010).
[28] R. R. Hartmann, J. Kono, and M. E. Portnoi, Nanotechnology **25**, 322001 (2014).

[29] S. A. Mikhailov, Phys. Rev. B **87**, 115405 (2013).
[30] A. Moskalenko and S. Mikhailov, J. Appl. Phys. **115**, 203110 (2014).
[31] T. Zhan, D. Han, X. Hu, X. Liu, S.-T. Chui, and J. Zi, Phys. Rev. B **89**, 245434 (2014).
[32] S. Liu, C. Zhang, M. Hu, X. Chen, P. Zhang, S. Gong, T. Zhao, and R. Zhong, Appl. Phys. Lett. **104**, 201104 (2014).
[33] N. R. Sadykov, E. A. Akhlyustina, and D. A. Peshkov, Theor. Math. Phys. **184**, 1163 (2015).
[34] N. R. Sadykov, A. V. Aporoski, and D. A. Peshkov, Opt. Quantum Electron. **48**, 358 (2016).
[35] Z. Yao, C. L. Kane, and C. Dekker, Phys. Rev. Lett. **84**, 2941 (2000).
[36] B. Q. Wei, R. Vajtai, and P. M. Ajayan, Appl. Phys. Lett. **79**, 1172 (2001).
[37] R. Murali, Y. Yang, K. Brenner, T. Beck, and J. D. Meindl, Appl. Phys. Lett. **94**, 243114 (2009).
[38] C. Berger, Y. Yi, Z. L. Wang, and W. A. de Heer, Appl. Phys. A **74**, 363 (2002).
[39] P. Poncharal, C. Berger, Y. Yi, Z. L. Wang, and W. A. de Heer, J. Phys. Chem. B **106**, 12104 (2002).
[40] C. Berger, P. Poncharal, Y. Yi, and W. A. de Heer, J. Nanosci. Nanotechnol. **3**, 171 (2003).
[41] Y. Yi, Ph.D. dissertation, Georgia Institute of Technology, 2004.
[42] J. Baringhaus, M. Ruan, F. Edler, A. Tejeda, M. Sicot, A. Taleb-Ibrahimi, A.-P. Li, Z. Jiang, E. H. Conrad, C. Berger *et al.*, Nature (London) **506**, 349 (2014).
[43] O. Klein, Z. Phys. **53**, 157 (1929).
[44] M. I. Katsnelson, K. S. Novoselov, and A. K. Geim, Nat. Phys. **2**, 620 (2006).
[45] I.-T. Lin and J.-M. Liu, Appl. Phys. Lett. **103**, 201104 (2013).
[46] P. Alonso-Gonzalez, A. Y. Nikitin, Y. Gao, A. Woessner, M. B. Lundeberg, A. Principi, N. Forcellin, W. Yan, S. Velez, A. J. Huber *et al.*, Nat. Nanotechnol. **12**, 31 (2016).
[47] K. Batrakov, P. Kuzhir, S. Maksimenko, A. Paddubskaya, S. Voronovich, P. Lambin, T. Kaplas, and Y. Svirko, Sci. Rep. **4**, 7191 (2014).
[48] K. Batrakov, P. Kuzhir, S. Maksimenko, A. Paddubskaya, S. Voronovich, G. Valusis, T. Kaplas, Y. Svirko, and P. Lambin, Appl. Phys. Lett. **108**, 123101 (2016).
[49] S. A. Mikhailov, in *Carbon Nanotubes and Graphene for Photonic Applications*, edited by S. Yamashita, Y. Saito, and J. H. Choi (Woodhead Publishing, Cambridge, U.K., 2013), Chap. 7, pp. 171–219.
[50] A. H. C. Neto, F. Guinea, N. M. R. Peres, K. S. Novoselov, and A. K. Geim, Rev. Mod. Phys. **81**, 109 (2009).
[51] S. Das Sarma and E. H. Hwang, Phys. Rev. Lett. **102**, 206412 (2009).
[52] E. M. Lifshitz and L. P. Pitaevskii, *Physical Kinetics*, 1st ed., Course of Theoretical Physics Vol. 10 (Pergamon, Oxford, U.K., 1981).
[53] S. A. Mikhailov and K. Ziegler, Phys. Rev. Lett. **99**, 016803 (2007).
[54] L. Schächter and A. Ron, Phys. Rev. A **40**, 876 (1989).